Energy Technology
Generation, Conversion, Storage, Distribution
www.entechnol.de

A General Technoeconomic Model for Evaluating Emerging Electrolytic Processes

*Michael J. Orella, Steven M. Brown, McLain E. Leonard, Yuriy Román-Leshkov, and Fikile R. Brushett**

Increasing societal concern about carbon emissions and the concomitant emergence of inexpensive renewable resources provide growing impetus for the electrification of the chemical industry. Despite notable advances in the science and engineering of electrolytic processes, there are comparatively few engineering economic studies that outline the technical specifications needed to approach feasibility. Herein, an open-source technoeconomic framework is introduced to quantify the economic potential of existing and conceptual electrolytic processes by connecting system price and performance goals with constituent materials property sets. To validate the outputs and demonstrate the versatility of this toolkit, three contemporary electrolyses of varying technology readiness levels are explored. Specifically, the model results are benchmarked against the Department of Energy hydrogen analysis model; the impact of mass transport and catalyst performance on the electrochemical reduction of carbon dioxide is evaluated; and a pathway to low-cost electrolytic production of phenol from guaiacol is charted. As this model is based on generalized mass balances and electrochemical equations common to a number of electrochemical processes, it serves as an adaptable toolkit for researchers to evaluate new chemistries and reactor configurations.

1. Introduction

Electrochemical technologies are poised to play a pivotal role[1–4] in enabling the use of low-cost intermittent renewable energy[5–10] to transform the global energy economy.[11,12] To date, most research efforts have focused on advancing electrochemical systems to serve as stationary energy storage, buffering power delivery from variable energy sources on the electric grid,[9,13–16] or displacing internal combustion engines in transportation.[17–20] However, efforts to develop electrochemical supplements to traditional chemical manufacturing have been less evident, despite the fact that the basic chemical and refining sectors were responsible for 26% of the global energy demand in 2012[12] and 32% of global carbon emissions in 2010.[21] The ability of traditional manufacturing to take advantage of renewable electrons to replace emission-intensive processes could begin reductions necessary in this sector to avoid the worst effects of climate change.[22]

Historically, innovations in electrochemical processing have lagged behind those in thermochemical processing in large part due to the high quality[23] of electrical energy as compared to thermal energy, leading to the economic impetus to use cheap energy sources over more expensive or unreliable ones.[1] However, as low-cost, renewable electricity shifts this paradigm,[24,25] opportunities emerge to explore the potential role of electrocatalytic processes, especially under conditions that challenge traditional processing strategies. Several possible advantages of electrochemical reactors include operation near ambient conditions, rapid dynamic response to start-up and shut-down, and innately tunable catalyst/electrode surface energy through varying potential, all of which, if realized together, may enable reaction pathways that were not previously attainable.[26] Accordingly, the effective application of electrocatalysis may both improve the sustainability of pre-existing manufacturing facilities and unlock exciting new chemistries that could foster the materials and fuels of the future. Indeed, among others, there are growing bodies of work around electrolytic hydrogen production,[27] the electrochemical reduction of carbon dioxide (CO_2) to a variety of useful products,[28–38] and the electrocatalytic upgrading of biomass-derived organics.[39–42] Although many of these scientific studies and resulting proof-of-principle devices hold promise, significant uncertainty remains around the ultimate performance, durability, and cost of these conceptual technologies.

As economic considerations drive technology adoption, the ability to connect system price targets to component performance parameters at an early stage is key to assessing concept feasibility, identifying technical obstacles, and, ultimately, allocating limited resources most effectively. Indeed, technoeconomic models of varying levels of detail and sophistication have been put forth to assess the merits of specific electrochemical technologies.[26,43–52] Most models focus on projecting prior performance data or reasonable predictions of improvement to a desired system price for a particular technology, rather than

M. J. Orella, Dr. S. M. Brown, M. E. Leonard, Prof. Y. Román-Leshkov, Prof. F. R. Brushett
Department of Chemical Engineering
Massachusetts Institute of Technology
77 Massachusetts Avenue, Cambridge, MA 02139, USA
E-mail: brushett@mit.edu

The ORCID identification number(s) for the author(s) of this article can be found under https://doi.org/10.1002/ente.201900994.

DOI: 10.1002/ente.201900994

attempting to translate targeted system prices to required materials performance metrics. In addition, to the best of our knowledge, no current model has been shown to be applicable to multiple electrocatalytic technologies, despite shared fundamental thermodynamic, kinetic, ohmic, and mass transfer processes described by the same set of constitutive relations. Accordingly, it is desirable to advance technoeconomic models that are flexible enough to provide insight into the interdependence of cost-constraining variables, thus illuminating pathways to cost reductions not apparent from the manipulations of individual variables. Such models should not only be widely applicable but also be generally accessible to the broader research community interested in electrochemical technology.

Herein, we present a general open-source MATLAB model for evaluating technoeconomic feasibility of generic electrolytic reaction schemes. This framework can describe multiple chemistries, is flexible enough to inform correlations between performance-defining variables, and is freely available to the research community for critical assessment, iterative improvement, and application-specific refinement. We intend this analytical framework to be useful in establishing design maps that identify performance benchmarks, highlight technical hurdles, and inform fundamental research into the chemistries, materials, and reactors needed for a viable technology platform. This framework is designed for the purpose of providing the preliminary analysis that is necessary before a more detailed technical evaluation of any specific process, and as such we rely on several simplifying assumptions that will need to be carefully considered for the process chemistry of interest. To first demonstrate the accuracy of our model, we show agreement between our results and those reported by the hydrogen analysis model (H2A) of the United States Department of Energy (US DOE) for the production of hydrogen via water electrolysis, despite differences in model specificity and formulation. We next establish the model generality by evaluating CO_2 reduction, where the production of carbon monoxide (CO) presents a well-studied model system within which we test the impacts of mass transport and catalyst performance. Finally, we show the utility of the model in exploratory systems such as electrocatalytic hydrogenation (ECH) by studying the trade-off between electrocatalyst selectivity and reactor operating conditions in the hypothetical production of phenol from guaiacol. Ultimately, we aim for this toolkit to be broadly accessible to the research community so that they may use it to study their own reaction systems of interest.

2. Model Description

In this section, we describe the governing equations and provide a summary of the simplifying assumptions that are used to represent the electrolysis system. We accomplish the goals described in the Introduction by drawing inspiration from a number of previous technoeconomic studies[43,53–56] on different electrochemical systems that sought to describe the connection between component materials and system characteristics. Incorporating these approaches, we are able to accurately simulate a wide range of chemistries and their economic feasibilities without requiring in-depth knowledge about the specifics of each process. Although this model can map the feasible design spaces and establish interdependencies between key variables, it does not consider the technical intricacies associated with traversals of this space. We envision that once the design space and key trade-offs are outlined, process-specific models can be used to refine the most-likely property sets for the associated chemistries. Importantly, there are certain relationships that are beyond the scope of the current model, such as the particular dependence of the boundary layer thickness within porous electrodes on the velocity of the reaction mixture within the electrolysis stack. For the interested reader, this modeling toolkit with corresponding cost and performance parameters can be freely accessed on GitHub[57] and a more detailed derivation is presented in the Supporting Information.

The process being modeled (**Figure 1**) can be broken down into several smaller subprocesses. The first block combines a fresh and recycled reactant (R), solvent, and electrolyte. After pretreatment, the reaction mixture is introduced into the

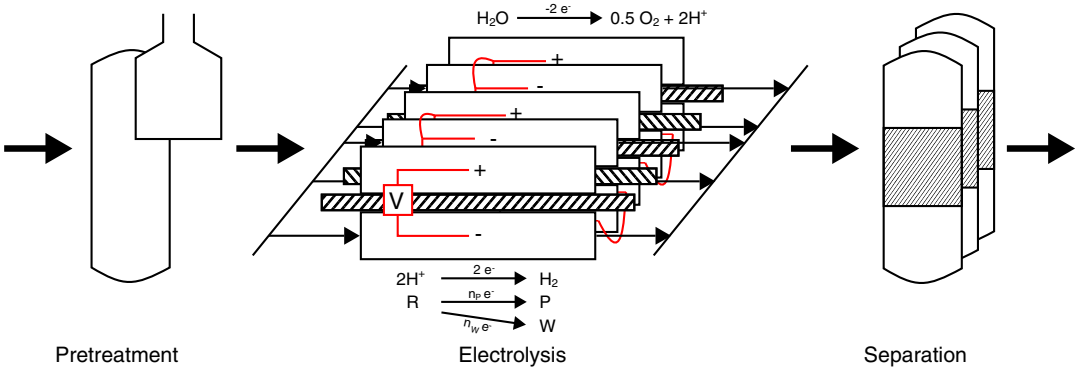

Figure 1. An overview of the process modeled. A fresh and recycled reactant is introduced to a pretreatment block from the far left, before continuing to an electrolysis stack, where each cell is connected electrically in series and hydraulically in parallel. Within the stack, the reactants are electrochemically reduced to either desired or waste products. In addition, hydrogen gas can be generated from the reduction of the protic electrolyte solution on the cathode. The oxygen evolution reaction is assumed to occur on the anode though other electrochemical oxidation reactions could be considered. Finally, the crude reaction products enter a separations train, where the desired products are separated to be sold, unreacted material is recycled, and undesired products are wasted.

electrolytic stack, where R is converted to a desired product (P) or to an undesired side product (W) in a parallel reaction. In addition to the parallel reaction network, any protic electrolyte solution in the presence of a cathode at a suitable reducing potential can undergo the parasitic hydrogen evolution reaction (HER), removing catalytically active hydrogen from the surface. The arrangement of the cells electrically in series but hydraulically in parallel within the stack was chosen as this configuration is most commonly used in industrial electrochemical applications.[58]

After the reaction mixture leaves the electrolysis stack, it enters the separations train, where unreacted material is separated from the products. For this analysis, we focus primarily on the electrolyzer stack operating at standard temperature and pressure, making simplifying assumptions about the overall process as well as contributions from the separations. First, the stack is assumed to operate at steady state and maintain a constant production rate throughout its operating lifetime such that no dynamics, replacement, or component performance decay need be considered. Second, the stack is operated in a galvanostatic manner such that requisite reaction areas and electrochemical kinetic requirements can be directly calculated. Third, we assume the only spatial gradients that exist within each cell arise from mass transfer boundary layers such that heat transfer need not be considered and mass transfer can be simplified to steady-state unidirectional diffusion. Fourth, heats of reaction are ignored such that each cell is operated in an isothermal manner. Fifth, cell separators and membranes are assumed to operate with perfect selectivity, such that there is no product or reactant crossover between the cathodic and anodic half-cells. Sixth, for this study we only consider the water oxidation reaction at the anode and do not deconvolute polarization losses associated with this reaction. Seventh, we assume that all separations costs can be described by Sherwood mass transfer correlations,[59,60] recognizing that although such correlations have been used previously,[43] they only provide order-of-magnitude estimations and likely underestimate the complex separations that accompany electrochemical processes. Eighth, we assume that the stack operates with perfect system efficiency, such that no losses arise from having multiple cells in series due to shunt currents or other inefficiencies. Finally, cost factors for the capital, balance of plant, and additional costs can be estimated from similar electrochemical technologies (see Supporting Information for additional details on estimated economies of scale).[55,56] Although we recognize the limitations, making these assumptions allows us to construct a conservative yet generalizable model using the limited economic data available in the open literature. Using the aforementioned assumptions, we develop a framework of mass balances, thermodynamics, kinetics, and mass transfer relations that can be summarized by the annualized cost to the consumer shown in Equation (1), which is the basis for all determinations of economic feasibility.

$$C = \frac{C_{\text{elec}} + C_{\pm} + \frac{C_{\text{cap}} + C_{\text{BOP}}}{\tau} + C_{\text{sep}}}{(1 - F_{\text{add}})\dot{N}_{\text{p}} M_{\text{p}}} \tag{1}$$

This minimum cost to the consumer (C) is a combination of operating expenses—electricity (C_{elec}) and materials ($C_{\pm}$)—and capital costs associated with the electrolyzer stack (C_{cap}) and pumps, heat exchangers, and piping associated with the electrolysis stack or pretreatment in the balance of plant (C_{BOP}), each of which is normalized by the operating lifetime of the plant (τ). The annualized separations costs (C_{sep}) are estimated from Sherwood correlations. The total costs contain additional economic factors such as labor costs, overhead, depreciation of any capital investments, and profit margins, which we assume to be a percentage of the total cost (F_{add}). This total cost is then normalized by the production rate ($\dot{N}_{\text{P}}$; mole per second) and molecular weight (M_{P}; gram per mole) to obtain the cost to the consumer in dollars per mass. The economic feasibility, or lack thereof, can simply be estimated by comparing the minimum cost to the consumer to current selling price of the desired product. To calculate each individual contribution to this total, the output set assignment is generated first (Table S2, Supporting Information). Of the 49 unknowns considered within the model, there are 15 equations relating their values by mass balances, constitutive relations, and component costs, resulting in 34 degrees of freedom through which the model may be parameterized. Equation (2)–(5) show the capital costs, balance of plant costs, electricity costs, and material costs, respectively.

$$C_{\text{cap}} = A_{\text{c}}(F_{\text{cap}} + \rho_{\text{cat}} F_{\text{cat}}) \tag{2}$$

$$C_{\text{BOP}} = A_{\text{c}} F_{\text{BOP}} \tag{3}$$

$$C_{\text{elec}} = IVP_{\text{elec}} \tag{4}$$

$$C_{\pm} = \dot{N}_{\text{R,f}} M_{\text{R}} P_{\text{R}} + \dot{N}_{\text{R,0}} \frac{1}{m_{\text{R}}} P_{\text{solv}}(1 - \phi_{\text{S}}) + \frac{-I}{F} r M_{\text{salt}} P_{\text{salt}}(1 - \phi_{\text{E}}) \tag{5}$$

The capital cost equation is informed by the H2A model from the US DOE[55,56] and redox flow battery modeling by Dmello et al.[53,54] where there is a fixed cost per electrolyzer area (F_{cap}), and the cost factor for the cathode electrocatalyst is considered separately to be a function of the catalyst specific price (F_{cat}; per mass) and specific loading (ρ_{cat}; mass per area). To obtain the total installed capital cost, these cost factors were weighted by the requisite electrolyzer area, which can be obtained from thermodynamics, kinetics, ohmics, mass transfer, and their constitutive relations (vide infra). The balance of plant is assumed to have the same scaling; namely, as the electrolyzer stack area increases, so too must the cost of the associated hardware as determined by its own areal factor (F_{BOP}).[55,56] Electricity cost contributions can be calculated using the present industrial electricity price (P_{elec}) and the necessary electrolyzer power draw, which can be determined from the product of the total current (I) and operating voltage (V). Finally, the material costs can be calculated as a sum of the necessary fresh reactant feed ($\dot{N}_{\text{R,f}}$), weighted by its molar mass (M_{R}) and price (P_{R}); the potentially required solvent as calculated by the reactant flow rate in the reactor inlet ($\dot{N}_{\text{R,0}}$) and its molality (m_{R}), the solvent price (P_{solv}), and the fraction of solvent that is recoverable by recycling (ϕ_{S}); and the amount of supporting electrolyte that may be necessary to add as a ratio to the amount of charge passed (r), the molar mass of the supporting electrolyte (M_{salt}), the price of the electrolyte (P_{salt}), and the fraction of recoverable electrolyte via

separation (ϕ_E). As the need for solvents or supporting electrolytes is reaction and device dependent, they can be incorporated or excluded as necessary, as explicitly documented in the case studies presented here. All feed cost contributions, consisting of the reactant, solvent, and supporting electrolyte, can be directly calculated from material balances around either the electrolyzer itself or the entire process. To obtain these material balances, we first consider the amount of reactant that must enter the reactor ($\dot{N}_{R,0}$), which can be calculated according to the conversion (χ), the total required current (I), the Faraday constant (F), the Faradaic efficiency (ε_i), and the number of electrons (n_i) involved in each reaction, as shown in Equation (6).

$$\dot{N}_{R,0} = -\frac{I}{\chi F}\left(\frac{\varepsilon_P}{n_P} + \frac{\varepsilon_W}{n_W}\right) \tag{6}$$

In the use of Faraday's law presented in Equation (6), we assume that the only three reactions that occur are the production of waste, desired product, and hydrogen, leading to a required unit sum of these Faradaic efficiencies. Although the reactant feed value is indirectly used to calculate the solvent requirements, as shown in the second term in Equation (5), the amount of fresh reactant ($\dot{N}_{R,f}$) can be reduced by recycling a known unreacted fraction (ϕ_R). The mass balance around the entire facility can be used to compute this fresh reactant feed rate, as shown by Equation (7).

$$\dot{N}_{R,f} = \dot{N}_{R,0}(1 - \phi_R(1 - \chi)) \tag{7}$$

The reactor area, which is the critical factor for determining capital costs, can be computed as the ratio of the total current requirement (I) to the applied current density (j). The total current that is passed can be computed from the fixed production rate ($\dot{N}_P$) and Faradaic efficiency (ε_P) by Faraday's law, as shown in Equation (8).

$$A_c = \frac{I}{j} = -\frac{\dot{N}_P n_P F}{j\varepsilon_P} \tag{8}$$

The final cost contribution to be defined is the electrical power draw (IV), as shown in Equation (4). As the total applied current has already been computed, the only remaining piece is the cell voltage (V). Based on the assumptions of stack efficiency, the total current and cell voltage can be used as a direct proxy for cell current and stack voltage, as the number of cells cancels from the power calculation. The total voltage drop across the cell can be described by the summation of the open circuit (thermodynamic) voltage (V_0) and the overpotentials due to kinetics (η_{kin}), ohmics (η_{ohm}), and mass transfer (η_{mt})— $V = V_0 + \eta_{kin} + \eta_{ohm} + \eta_{mt}$. The thermodynamic voltage can be computed from the difference in standard reduction potentials of the two half reactions (V^θ) and reactant concentrations according to the Nernst equation, shown in Equation (9). As shown in the Supporting Information, we assume unit activity coefficient for all reacting species.

$$V_0 = V^\theta + \frac{RT}{n_P F}\ln\left(\frac{1-\chi}{\chi\varepsilon_P}\right) \tag{9}$$

The ohmic overpotential is perhaps the most readily calculated as the only requisite information is the ionic conductivity of the medium (σ) and the distance separating the two electrodes (L_c), from which Ohm's law can be used, $\eta_{ohm} = j\frac{L_c}{\sigma}$. The kinetic overpotentials can be calculated from any appropriate electrochemical kinetic theory, but for this implementation of the model we elect to use Butler–Volmer kinetics, which is parameterized by a charge transfer coefficient (α) and an exchange current density (j_0), as shown in Equation (10).

$$j = j_0\left(\exp\left(-\frac{\alpha\eta_{kin}n_P F}{RT}\right) - \exp\left(\frac{(1-\alpha)\eta_{kin}n_P F}{RT}\right)\right) \tag{10}$$

Finally, considering the complex topographies of most real electrodes, we begin the analysis of mass transfer by considering the steady-state diffusion of species described by a molecular diffusion coefficient (D) to a planar electrode across a boundary layer of certain thickness (δ). Accordingly, the limiting current density (j_{lim}) and corresponding mass transfer overpotentials can be computed using Equation (11).

$$j_{lim} = -\frac{n_P F D C_{R,f}(1-\chi)}{\delta}, \quad \eta_{mt} = \frac{RT}{n_P F}\ln\left(1 - \frac{j}{j_{lim}}\right) \tag{11}$$

As stated earlier, the primary focus of this model is the physical description of the reaction and transport processes within the electrolyzer itself. However, the relative cost and performance of the separations can significantly impact reactor performance or operating conditions; thus, it is necessary to consider separations in any reactor model, even if only from an order-of-magnitude perspective. In the Sherwood plot shown in Dahmus and Gutowski,[59] there are three classes of materials presented that are all found to fit different lines of the form $P_{sep} = k_P/w_i$, where P_{sep} is the separation price, w_i is the initial concentration, and k_P is the separation factor in dollars per kilogram of total mixture passing through the separations train. By fitting these data, the authors were able to obtain separation factors of \$1 kg^{-1} of initial mixture for separating biologics, \$0.01 kg^{-1} of initial mixture for separating metals, and \$0.001 kg^{-1} of initial mixture for separating gases. The separations costs can then be roughly approximated as the product of these factors and the total mass flow rate through the separations train.

To this point, there have been no assumptions of specific materials properties that are used within the electrolytic stack or as feed or product. Instead, we rely on the specification of independent model parameters to identify these cases. As with all economic models, parameter uncertainty can have significant implications on one's ability to draw conclusions, which can be especially daunting in the case of evaluating new technologies. However, by examining the trends that may be established through these types of models with standard sensitivity analysis (vide infra) or by using a more complex Monte Carlo approach (Figure S2 and S3, Supporting Information), researchers can establish bounds upon which they may be able to draw their own conclusions.

For researchers to evaluate chemistries of their own interest, the model can be run by modifying any subset of these model parameters and constructing an instance of the "EconomicCase" object available on GitHub. The model is run

through the construction process, which can be verified by examining the "cost" property of the constructed object. Through this approach, we generated a simple toolkit for understanding the physical bounds of the economically viable operating space. The ability to identify the shape of this space allows a more direct translation of system price targets to requisite materials performance targets, illuminating the most pressing technical challenges.

3. Results and Discussion

As described in the previous section, we established a general framework for evaluating the economic feasibility of reductive electrocatalytic reactions. Although a full parametric sweep of the 34D operating space is impractical, it is nevertheless useful to both validate and demonstrate the current model against both established and hypothetical technologies, with a focus on pertinent sets of interdependent cost-constraining variables. Instead of attempting to visualize the full operating space, we project into 1 or 2D space and examine the interdependencies between subsets of relevant variables and parameters. To that end, we report the usage of the model through three case studies: water electrolysis to generate hydrogen (**Scheme 1**a), CO production through reduction of CO_2 (Scheme 1b), and phenol production through the ECH of guaiacol (Scheme 1c).

3.1. Comparison of Current Work to US DOE H2A Model

Water electrolysis to generate molecular hydrogen is emerging as a promising approach to improve the sustainability of the chemical industry.[27] Hydrogenations, which underpin many important chemical processes, rely on steam methane reforming, or other such reforming reactions, followed by compression in capital-intensive turbines to generate the necessary supply of high-pressure hydrogen.[61] Water electrolyzers have the potential to harness renewable electricity to generate pressurized hydrogen feeds, avoiding additional capital-intensive processing steps.[27] However, high electricity costs and expensive catalytic materials have thus far limited technology adoption in favor of the significantly cheaper hydrocarbon reforming processes. Advancing new catalysts, engineering improved reactor designs, realizing economies of scale, and decreasing electricity costs will each contribute to increasing the cost competitiveness of electrolytic hydrogen generation.[55,56]

To evaluate the accuracy of the present model, we benchmark our results for water electrolysis against the established H2A model[55,56] at two production scales (1500 kg day^{-1} forecourt to 50 000 kg day^{-1} central) and show that despite the lack of chemical specificity, the current framework can accurately predict cost behavior (**Figure 2**). First, in both cases, the cost of electricity dominates the price of hydrogen electrolysis. This scaling of the electricity cost is largely due to the low molecular weight of hydrogen, necessitating high specific power for economic viability. This is motivating research efforts toward increasing the power density while decreasing the overall power consumption of water electrolyzers.[62] The additional costs, balance of plant, and capital cost factors were all matched to the hydrogen cost parameters for this study, leading to nearly identical behavior between the two models. In both models, the feed is treated as process water, which makes up a negligible fraction of the total hydrogen cost. Per assumption six (vide supra), we assume that the catalyst costs for any HER or water oxidation materials are incorporated in the capital costs. Finally, it is worthwhile to consider the effects of electrolysis cost across different scales. From the H2A data, there appear to be no significant economies of scale, which subsequently translates to the current model as the capital cost factors having little sensitivity to the product throughput. However, the extent to which economies of scale reduce production costs remains unclear as few electrochemical systems are manufactured at the scale of their thermochemical analogues.[63]

Although the total costs appear to appropriately verify the model, it is perhaps more important that the model predicts the correct response to variations in parameter values as shown in Figure 2b. A more complete evaluation of the most sensitive model parameters using Monte Carlo simulations is shown in Figure S2, Supporting Information. Although these sensitivity

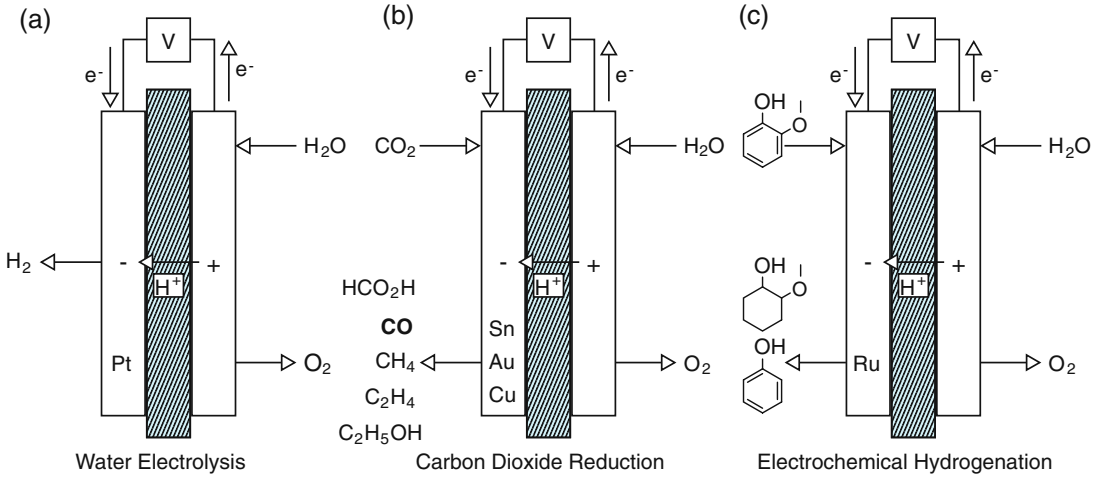

Scheme 1. Simplified representations of electrolytic production of a) hydrogen from water, b) carbon monoxide from carbon dioxide, and c) phenol from guaiacol via a two-electron reduction with a possible unwanted six-electron over-reduction to 2-methoxy-cyclohexanol.

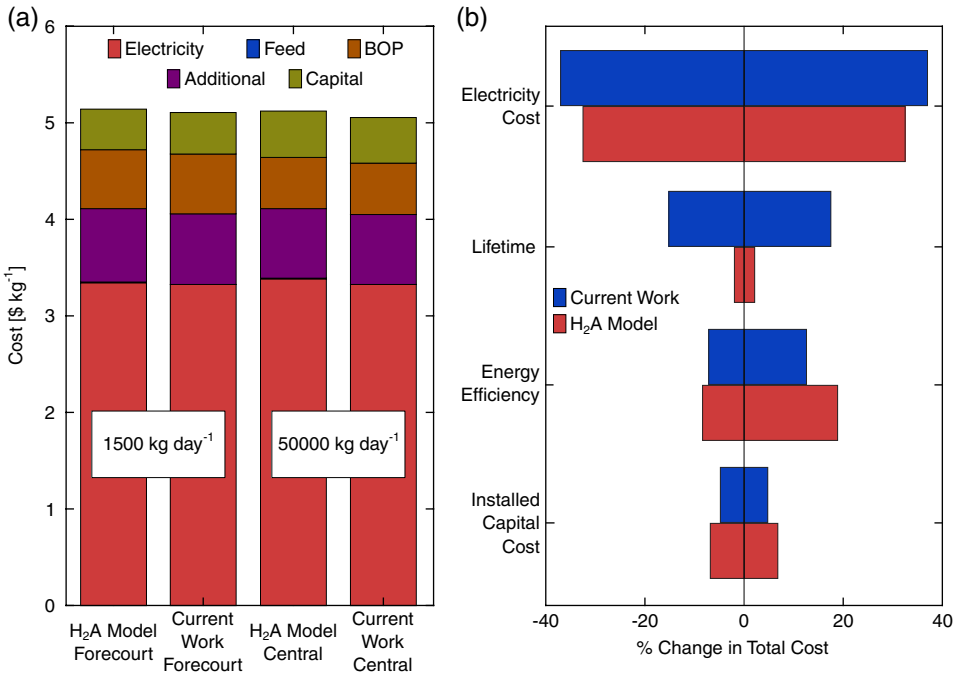

Figure 2. Direct comparison between the US DOE H2A results and the proposed model's results. a) At two production scales, the model shows quantitative agreement. b) Sensitivity of the model to parameters as reported by the current model and by the US DOE using parameter bounds reported by US DOE.

analyses do not serve as appropriate risk assessment metrics at present, similar strategies could be used with detailed probability density functions for each parameter to derive the likelihood of particular hydrogen production costs. Although there is general agreement across multiple parameters, a key discrepancy in model sensitivities is the treatment of system lifetime. Upon deeper inspection of the H2A model, aggressive salvage of the electrolytic system is anticipated. However, as electrochemical systems at scale have not yet been deployed from which salvage values can be extracted, we opt to examine the extreme case of obtaining no salvage value from the capital purchase. In this limiting case, we may overestimate the impact of the system lifetime, but based on the lack of clarity in the H2A model, this approach provides the most conservative estimate of the process economics.

3.2. The Impact of Mass Transfer and Catalyst Performance on CO_2 Reduction

One of the most studied electrolytic reactions over the last decade is the electrochemical reduction of CO_2, which has potential value as a method for carbon-neutral fuel production or waste stream valorization, depending on the electrocatalyst used and electrolysis conditions. Concerted efforts on catalyst development have led to the generation of two-electron reduction products such as CO and formate at Faradiac efficiencies that approach and surpass 95% as well as steady advances in the selective generation of more deeply reduced products.[26] However, a number of scientific and engineering challenges remain for the commercialization of CO_2 reduction,[36,64–66] for example, the successful incorporation of highly engineered catalysts into high-surface-area electrodes that are stable over the reactor lifetime.[64] Despite these hurdles, a number of start-ups are taking innovative approaches to developing economically feasible and large-scale CO_2 reduction.[31]

Although well-founded CO_2 reduction economic models exist in the literature,[26,43,67] several important questions persist for the general design space for CO_2 electrolysis. First, from the suite of possible products that can be made from CO_2 reduction, which is the most promising? Second, what feed source of the CO_2 should be used for electrochemical reduction? Third, what are the trade-offs in catalyst material choice in the importance of activity and selectivity? Using our model, we can begin to address these questions at a high level, outlining the shape of the design space for these devices and developing the intuition necessary to better design future electrolytic processes.

The cost to the consumer of CO, formate, methane (CH_4), ethylene (C_2H_4), and ethanol (C_2H_5OH) based on the model predictions shown in **Figure 3** suggest the economic feasibility of CO production from CO_2. For each of these reactions, water oxidation with no catalyst beyond that considered in the hydrogen production case was assumed to take place at the anode, whereas an additional catalyst layer was considered for each of the different reaction products on the cathode. In these estimates, gaseous CO, methane, and ethylene were assumed to be generated without a supporting electrolyte or solvent in the reactant or product streams, whereas liquid formic acid and ethanol were generated in the presence of a carrier solvent without electrolyte that could remove them from the electrolysis reactor. From these cost breakdowns, the number of electrons necessary to produce CH_4, C_2H_4, and C_2H_5OH makes electrical costs a significant contribution to the total cost. Consequently, there are

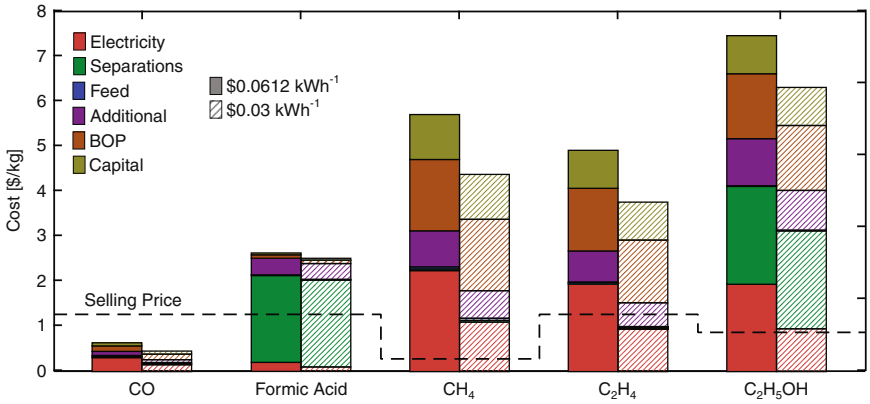

Figure 3. The cost breakdown of CO_2 reduction technology to a variety of different products including CO, formic acid, methane (CH_4), ethylene (C_2H_4), and ethanol (C_2H_5OH). Each bar contains cost components from electrical power, separations, electrolyte, additions to the total cost, balance of plant, and capital investment. The bars on the left use the parameters described in Table S2, Supporting Information, with an electricity price of \$0.0612 kWh^{-1}, whereas the hashed bars use an electricity price of \$0.03 kWh^{-1} based on predictions of future electricity prices.[25]

correspondingly high capital and balance-of-plant costs. Although the electric and capital requirements for both CO and formic acid appear promising, the added difficulty in the liquid separation adds a significant cost to formic acid production. To estimate the separations cost, we use separation factors of \$0.003 kg^{-1} of mixture for all gas separations and \$0.4 kg^{-1} of mixture for all liquid separations. Although data for nonbiologic liquid products were not found in published Sherwood charts, we assume these separations would be about one order of magnitude less expensive. The cost of these separations was verified by more rigorous analysis of the distillation train using Aspen Plus simulations (see Supporting Information). In each of these estimated separation factors, the factor of either 3 or 4 arises from the number of components (reactant, product, waste, and potentially solvent) that must be separated from the crude reaction stream. For this analysis, we only consider separations of products in the same physical phase, treating all secondary products in that phase as a single waste stream. We note that for these separations estimates, the separation cost is directly correlated to the separation factor, indicating that any change in the difficulty of the separation impacts the separation cost in the same way and that future iterations of the model examining different process chemistries will need to adjust this parameter to reflect the number of desired product streams. We compare these costs to the consumer with the average selling prices as reported by Verma et al.[43] and show quantitatively that CO can be produced in an economically feasible manner with current material performance. However, there is still a significant gap to overcome to synthesize methane (CH_4), ethylene (C_2H_4), and ethanol (C_2H_5OH) due to either the natural abundance of the desired product or inexpensive thermochemical alternatives for its production. In addition, due to the significant current requirements, even if electricity prices were to decrease from \$0.0612 to \$0.03 kWh^{-1}[25] and separations costs could be drastically decreased, the capital and balance-of-plant requirements still make these products economically infeasible with present technology. Note that we do not consider carbon taxes in this analysis but recognize that additional incentives to process CO_2 to more valuable materials could offset some of these economic penalties. In addition, here we only consider direct electrochemical transformations as opposed to more sophisticated tandem electrochemical/thermochemical systems. Such tandem systems could be easily studied using these types of general economic frameworks, if desired. For the remainder of this section, we focus on CO production as it is potentially profitable, as others have previously noted.[26,43]

The feed concentration required for an economically viable CO_2 reduction process determines the feasibility of different feedstocks as well as the scale of any necessary preconcentration steps. Also important to the process operation is the conversion per pass, as this value has a significant impact on the composition of the reactor exit stream and direct implications for the difficulty of the separations. To a rough approximation, Sherwood plots have been used in prior literature for calculating the cost of separations technologies, each of which scales with the mixture throughput.[43,59,60] In this case, as per-pass conversion decreases, both the separations costs and reactant concentrations increase, as a low conversion indicates that there is more unreacted material in the bulk fluid, which necessitates more material passing through the separations train. Our model suggests that minimum reactor feed CO_2 concentrations of ≈18% v/v are necessary, with separation costs becoming insignificant at conversions greater than ≈40% (**Figure 4**). This is in agreement with the work published by Pletcher, who postulated that CO_2 electrolysis would likely need significant preconcentration before it could be reacted in an electrolyzer.[67] At less than ≈18% and high current densities, the bulk concentration is too low to support access of the CO_2 gas to the electrocatalyst within the electrode, causing mass transfer limitations which necessitate larger reactors and increased cost. Enabling efficient operation at low feed concentrations would require advances in electrode design or manipulation of mass transport characteristics to either increase the effective diffusion coefficient or decrease the boundary layer thickness. Similarly, there are diminishing returns on any per-pass conversions above ≈40%, as, at this point, the costs of separations are negligible compared to more significant contributions such as electrical power and reactor capital. In addition, operating at higher

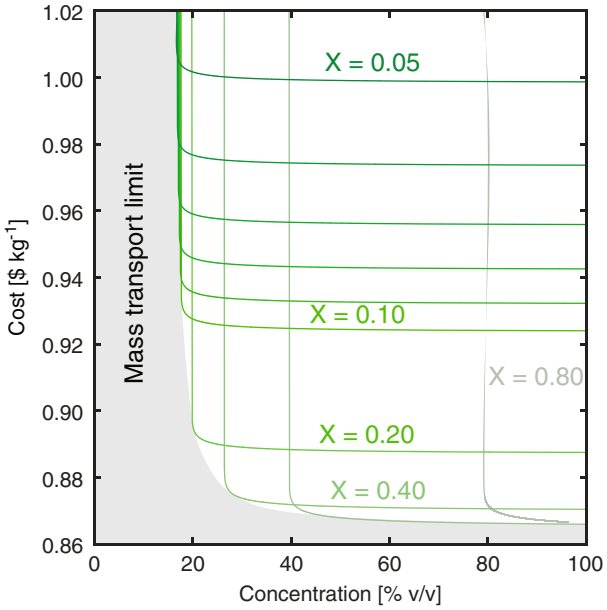

Figure 4. The impact of mass transfer and separations on the cost of reducing CO_2 can be significant. As the single-pass conversion inside the electrolyzer changes, there is a sharp mass transfer limit that cannot be surpassed, which effectively limits the feed concentration of CO_2 to the unit. The shaded contours represent different per-pass conversions (χ).

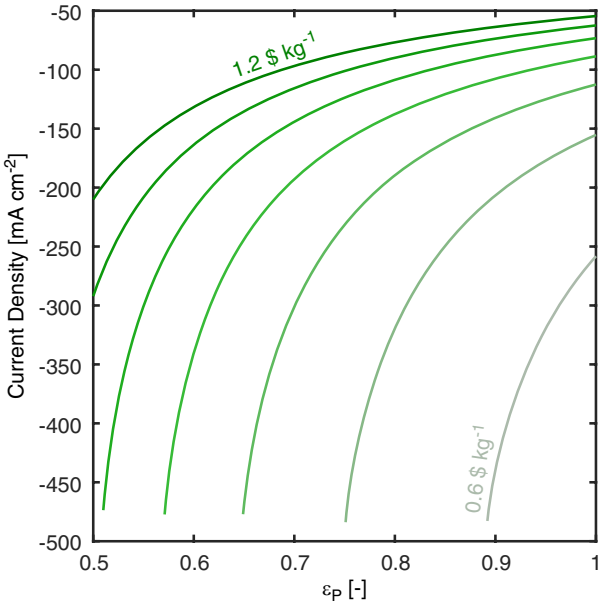

Figure 5. Design space for catalysts in CO_2 reduction to CO. As the catalyst selectivity decreases, activity must increase to maintain productivity, thus necessitating higher current densities. Mass transfer limitations set a lower bound on the allowable Faradaic efficiencies. As the total cost to the consumer decreases, the requirements on catalyst activity and efficiency get more stringent, as indicated by increasing minimum Faradaic efficiencies. The shaded contours represent different product costs.

conversions necessitates higher purity feeds, as the bulk concentration will deplete to the point of slowing mass transfer processes. Notably, we do not account for any impacts that chemical impurities in the feedstocks may have on either reactor or separations performance in this analysis.

One of the most pressing questions for CO_2 electrolysis surrounds the trade-offs between catalyst productivity and selectivity in a single material. To wit, for a particular catalyst, what is the necessary activity and selectivity to achieve particular system cost targets? Here, to explicitly evaluate the trade-offs that exist, we set a cost to the consumer and assess the required selectivity at any given activity. **Figure 5** shows contours of isocost with the requisite electrolyzer current draw and efficiency needed to achieve the specified cost targets. As the total cost to the consumer is increased, the range of acceptable materials widens as these can have lower activity and selectivity.

The interplay between the applied current density and electrocatalyst Faradaic efficiency can be observed along a contour. As the Faradaic efficiency decreases, the total current requirement must increase to keep the production rate fixed, which necessitates higher applied current densities to prevent increases in capital requirements and electrical power costs. Mass transfer rates of CO_2 to the electrode surface set an upper limit of achievable current density, as the reactant surface concentrations approach zero. This, in turn, establishes a minimum acceptable Faradaic efficiency, which adjusts with the minimum allowable cost to the consumer. It is also important to note the contraction of the design space that occurs from decreasing cost to the consumer, which both increases the minimum Faradaic efficiency and minimum current density that must be achieved in any reactor. Promisingly, however, we see that the required current density and selectivity have been achieved in synthetically accessible catalytic materials and advanced reactor systems, albeit for shorter operating times and in smaller formats than ultimately necessary.[31]

3.3. Investigation of Catalyst and Reactor Trade-Offs in Guaiacol Electrocatalytic Hydrogenation

Although less studied than H_2 evolution and CO_2 reduction reactions, ECHs are a growing area of electrolyses that hold promise for the sustainable production of more complex chemicals and fuels. ECH differs from electrolytic hydrogen production in that hydrogen adatoms that are electrochemically generated in situ from protic media react with the electroactive unsaturated reactant. Several proof-of-principle examples of such processes include ECH on sugar-derived platform chemicals,[68–72] biomass pyrolysis products,[39,41,73,74] and even unsaturated hydrocarbon gases.[75] Due to the dearth of technoeconomic studies beyond large-scale life-cycle analyses[76] as compared to other electrochemical technologies, we articulate general performance benchmarks representative of cost-effective ECH using the production of phenol from guaiacol, a popular model of depolymerized lignin found in pyrolysis oil,[40,74] as an example transformation. The molecular structure of guaiacol is nearly identical to that of phenol, only containing an additional methoxy group at the *ortho* position to the hydroxyl group. As phenol is a highly

valued material with significant market sizes, the ability to electrochemically cleave the methoxy group from the guaiacol, without hydrogenating the aromatic ring, would be highly desirable. Despite demonstrations indicating partial reaction of guaiacol to form phenol,[40,41,74] multiple questions remain regarding the optimal reactor geometry and requisite catalyst performance for cost-competitive processing. Therefore, to identify the operating space for electrolyzers and electrocatalysts, we examine the isoefficiency curves shown in **Figure 6**, assuming process water as a solvent and a supporting electrolyte to aid ionic conductivity. In addition, we again consider only water oxidation occurring at the anode and a catalyst layer on the cathode to promote the reactions of interest. In these curves, the Faradaic efficiency toward the HER, where the hydrogen adatoms on the surface combine to form molecular hydrogen gas rather than entering the organic reaction network, is varied within a particular color value, while the hues identify distinct selectivities between the cleavage of the methoxy group via hydrogenolysis and the saturation of the aromatic ring. For example, within all purple lines the total cost to the consumer at different applied current densities can be observed at a 12% selectivity within the organic network. As the saturation value of these lines decreases (i.e., becomes more gray), the total cost to the consumer decreases as the electrocatalyst becomes better at suppressing HER and therefore more effectively uses the provided electricity. By examining different organic network selectivities, which are represented by the uniquely colored panels in Figure 6, we can directly observe the interplay between the three relevant catalyst variables of organic reaction selectivity, HER Faradaic efficiency, and electrocatalyst activity.

These design space maps show qualitatively that it is more important to have an electrocatalyst that can minimize the HER than to have one that is selective within the organic network. There is a minimum reaction selectivity, ≈24%, in terms of electronic currents within the organic network that must be maintained to drive the production costs below about $\$1.30\,kg^{-1}$, which was approximately the global spot price in 2018.[77] Indeed, product selectivities above ≈50% do not appear to offer significant economic gains, whereas HER Faradaic efficiencies above ≈20% at 24% product selectivity precludes economic feasibility even in the case of highly active catalysts. Interestingly, the minimum electrocatalyst activity can be

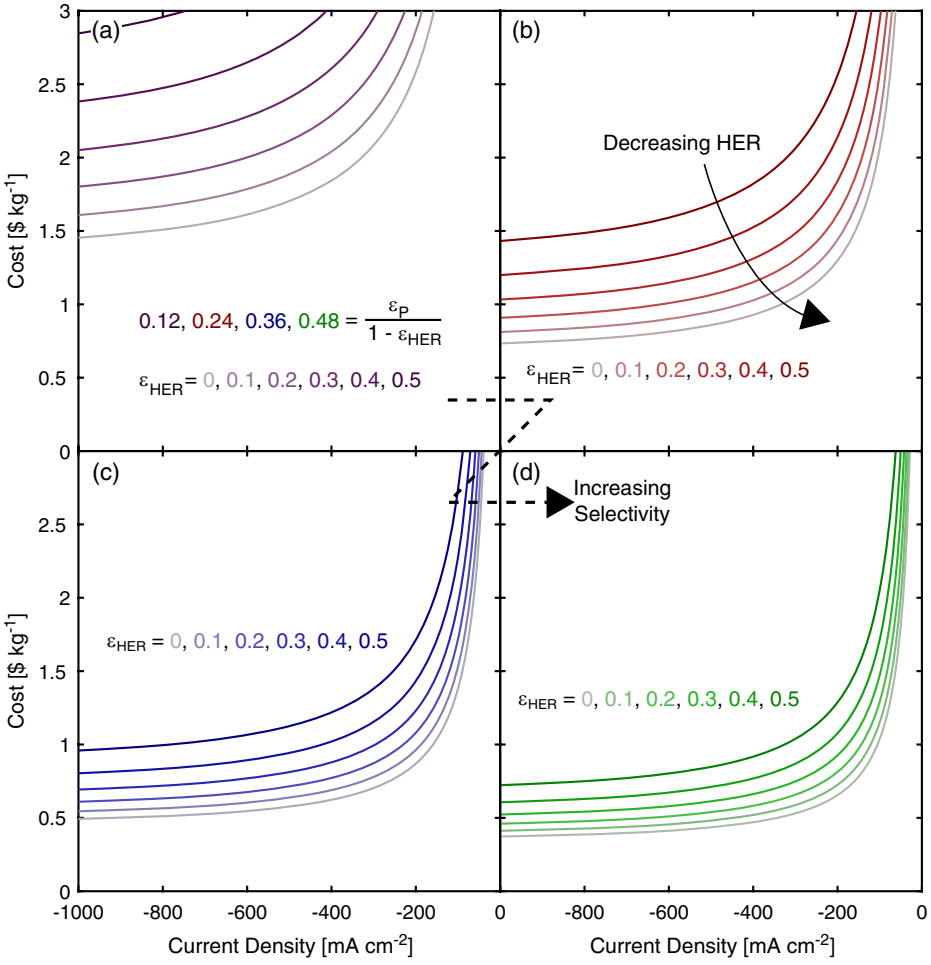

Figure 6. The sensitivity of phenol production cost to catalyst selectivity and activity. a–d) Different product selectivities are indicated by different colored lines, while lines of different intensity within each color scheme show the impact of parasitic hydrogen evolution on the selling price. As lines move toward the bottom right-hand side of the charts, the product efficiency increases whereas the HER efficiency decreases.

identified from the case of perfect selectivity toward our desired product. Given the aforementioned spot price, this would necessitate a current density of nearly 150 mA cm^{-2}, which may be feasible based on prior work in nonaqueous or mixed media.[78] Although these representations provide valuable insight into relationships between different material properties, it is more difficult to outline likely roadmaps to economic viability through sequential advances in this fashion. Instead, we employ a waterfall analysis shown in **Figure 7** to highlight the effects of cumulative technology improvements derived from the previous sensitivity analyses. The data for the base case were obtained from experiments performed by Saffron and coworkers in unoptimized H-type electroanalytical cells.[40,74] The authors reported phenol and hydrogen Faradaic efficiencies of 6% and 75%, respectively. Based on the difficulty of measuring electrochemically active surface area, only the total currents were reported, but by approximating the geometric area of the electrode, we estimate the applied current density to be near 50 mA cm^{-2}. With these parameters and estimates of other parameters that were not explicitly measured (Table S4, Supporting Information), we generate the base case shown on the far left of Figure 7. The first improvement, based on the sensitivity analysis shown in Figure 6, is an increase in the current density from 50 to 200 mA cm^{-2}, potentially enabled by advances in catalyst material, electrode fabrication, or cell format, resulting in a cost decrease of \$18.53 kg^{-1}. Next, we assume enhancements in catalyst selectivity such that the Faradaic efficiency of hydrogen generation decreases from 75% to 20%, which further reduces the cost to \$6.93 kg^{-1}. Finally, we assume the catalyst selectivity within the organic reaction network increases such that the Faradaic efficiency of the final product is 75%, a significant increase from the 6% reported,[40,74] leading to a final phenol production cost of \$0.42 kg^{-1}. However, should such an improvement prove unattainable, a target product Faradaic efficiency of ≈24% would enable production at equivalent to the current phenol spot price, as observed in Figure 6.

These analyses help to illustrate pathways to economical production of valuable chemicals via electrocatalytic technologies, but do not indicate that the technology yet exists to perform such electrolyses at scale. To that end, a significant amount of work is still needed before the benefits of such technologies can be realized. Based on the presented analysis, developing catalytic materials, electrodes, and reactors that can support high current density, suppress HER, and remain selective to the desired product remains of paramount importance. However, this particular pathway to economic feasibility is simply a demonstration and others may emerge with technical advances. These new pathways may be mapped in a similar manner. Finally, in this analysis, for the sake of clarity, we exclude the influence of separations but note that they will impact the overall feasibility of ECH processes.

4. Conclusion

Here we introduced a general model of thermodynamics, kinetics, ohmics, and mass transfer for evaluating the economic feasibility of electrocatalytic production of a wide variety of materials. First, we established the accuracy of the present model by comparing the US DOE H2A model results to the predictions that our model makes on the electrocatalytic production of hydrogen. Next, we examined the model outputs of the electrochemical reduction of CO_2 to CO, specifically with regard to the trade-offs in mass transfer and catalyst performance. Finally, we showed a theoretical pathway to low-cost electrocatalytic phenol production from guaiacol, which has yet to be experimentally realized but can help guide future materials research. Through contemplation of these case studies, we hope that the reader can take advantage of the generality of this model and use it to evaluate electrolytic technologies and guide future research in electrolytic reactions of interest. However, as individual projects garner deeper interest from a promising result using this model, additional economic and engineering complexities must be more deeply considered. First, a more detailed treatment of the necessary separations processes is important for strengthening physical connections between the reactor and separations performance. Second, more rigorous economic metrics need to be

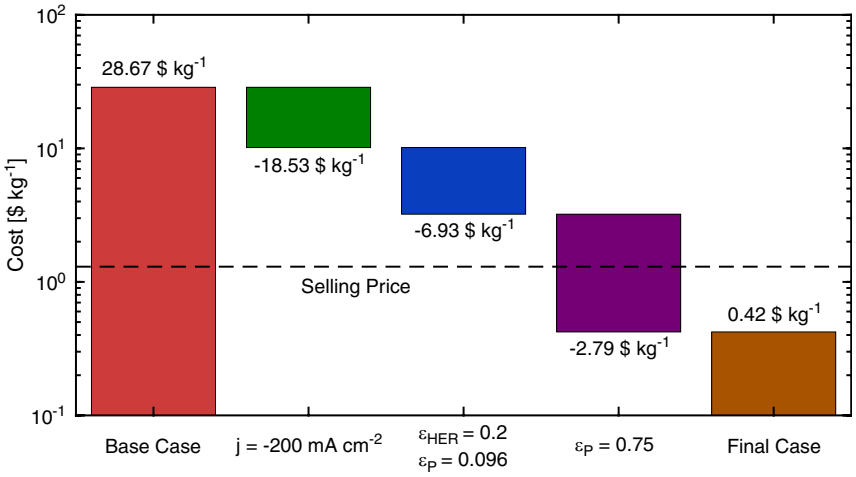

Figure 7. Waterfall chart detailing the possible engineering improvements that could be made to the production of phenol electrochemically. Given improvements in catalyst activity and selectivity, and reducing the propensity for hydrogen evolution, phenol could theoretically be produced at prices well below its current spot price.

incorporated that can be used to compare against alternative capital projects being considered by a manufacturer. Third and finally, more realistic descriptions of the physical processes within the electrochemical reactor would likely improve the accuracy of performance predictions, albeit at the expense of model simplicity and generality. Indeed, chemistry-specific deviations to a typical cell architecture may impact many of the relationships developed here, which must be considered once initial economic feasibility metrics are met, but such specifics are beyond the intended scope of this initial assessment. Through this toolkit of electrochemical engineering economics, researchers will now have a straightforward way of identifying economically feasible chemistries and identifying the most pressing economic challenges at the highest level of analysis.

Supporting Information

Supporting Information is available from the Wiley Online Library or from the author.

Acknowledgements

The authors gratefully acknowledge the National Science Foundation Graduate Research Fellowships Program under Grant No. 1122374 for support of M.J.O. Any opinions, findings, and conclusions or recommendations expressed in this material are those of the authors and do not necessarily reflect the views of the National Science Foundation. Additionally, this work was supported by research funding from the Massachusetts Institute of Technology. The authors thank Michael Stone for insightful discussion and constructive feedback.

Conflict of Interest

The authors declare no conflicts of interest.

Keywords

carbon dioxide reduction, electrocatalysis, electrocatalytic hydrogenation, technoeconomic model, water electrolysis

Received: August 19, 2019
Revised: November 25, 2019
Published online: December 27, 2019

[1] M. J. Orella, Y. Román-Leshkov, F. R. Brushett, *Curr. Opin. Chem. Eng.* **2018**, *20*, 159.
[2] E. J. Horn, B. R. Rosen, P. S. Baran, *ACS Cent. Sci.* **2016**, *2*, 302.
[3] J. Carneiro, E. Nikolla, *Annu. Rev. Chem. Biomol. Eng.* **2019**, *10*, 85.
[4] P. D. Luna, C. Hahn, D. Higgins, S. A. Jaffer, T. F. Jaramillo, E. H. Sargent, *Science* **2019**, *364*, eaav3506.
[5] M. Armand, J.-M. Tarascon, *Nature* **2008**, *451*, 652.
[6] J. B. Goodenough, Y. Kim, *Chem. Mater.* **2010**, *22*, 587.
[7] J.-M. Tarascon, M. Armand, *Nature* **2010**, *414*, 359.
[8] S. Teleke, M. E. Baran, S. Bhattacharya, A. Q. Huang, *IEEE Trans. Sustainable Energy* **2010**, *1*, 117.
[9] B. Dunn, H. Kamath, J.-M. Tarascon, *Science* **2011**, *334*, 928.
[10] D. Larcher, J.-M. Tarascon, *Nat. Chem.* **2015**, *7*, 19.
[11] J. M. Griffin, A.-M. Fantini, M. Tallett, R. F. Aguilera, J. L. Arellano, J. Ban, *World Oil Outlook 2015*, Organization of Petroleum Exporting Countries, Vienna **2015**.
[12] J. Conti, P. Holtberg, J. Diefenderfer, A. LaRose, J. T. Turnure, L. Westfall, *International Energy Outlook*, DOE/EIA-0484 (2016), US Energy Information Administration, Washington, DC **2016**.
[13] D. H. Doughty, P. C. Butler, A. A. Akhil, N. H. Clark, J. D. Boyes, *Electrochem. Soc. Interface* **2010**, *19*, 49.
[14] K. T. Cho, P. Albertus, V. Battaglia, A. Kojic, V. Srinivasan, A. Z. Weber, *Energy Technol.* **2013**, *1*, 596.
[15] P. Alotto, M. Guarnieri, F. Moro, *Renewable Sustainable Energy Rev.* **2014**, *29*, 325.
[16] M. A. Pellow, C. J. M. Emmott, C. J. Barnhart, S. M. Benson, *Energy Environ. Sci.* **2015**, *8*, 1938.
[17] C. E. Thomas, *Int. J. Hydrogen Energy* **2009**, *34*, 6005.
[18] B. Nykvist, M. Nilsson, *Nat. Clim. Change* **2015**, *5*, 329.
[19] J. Hagman, S. Ritzén, J. J. Stier, Y. Susilo, *Res. Transport. Bus Manag.* **2016**, *18*, 11.
[20] A. Mahmoudzadeh Andwari, A. Pesiridis, S. Rajoo, R. Martinez-Botas, V. Esfahanian, *Renewable Sustainable Energy Rev.* **2017**, *78*, 414.
[21] IPCC, *Climate Change 2014: Synthesis Report* (Eds: Core Writing Team, R. K. Pachauri, L. Mayer), IPCC, Geneva, Switzerland **2015**.
[22] IPCC, *Global Warming of 1.5°C. An IPCC Special Report on the Impacts of Global Warming of 1.5°C above Pre-Industrial Levels and Related Global Greenhouse Gas Emission Pathways, in the Context of Strengthening the Global Response to the Threat of Climate Change, Sustainable Development, and Efforts to Eradicate Poverty*, IPCC, Geneva **2018**.
[23] M. T. Brown, S. Ulgiati, *Ecol. Model.* **2004**, *178*, 201.
[24] R. Schmalensee, V. Bulovic, R. Armstrong, C. Batlle, P. Brown, J. Deutch, H. Jacoby, R. Jaffe, J. Jean, R. Miller, F. O'Sullivan, J. Parsons, J. I. Pérez-Arriaga, N. Seifkar, R. Stoner, C. Vergara, *The Future of Solar Energy: An Interdisciplinary MIT Study*, MIT Energy Initiative, Massachusetts Institute of Technology, Cambridge, MA **2015**.
[25] N. M. Haegel, R. Margolis, T. Buonassisi, D. Feldman, A. Froitzheim, R. Garabedian, M. Green, S. Glunz, H.-M. Henning, B. Holder, I. Kaizuka, B. Kroposki, K. Matsubara, S. Niki, K. Sakurai, R. A. Schindler, W. Tumas, E. R. Weber, G. Wilson, M. Woodhouse, S. Kurtz, *Science* **2017**, *356*, 141.
[26] M. Jouny, W. Luc, F. Jiao, *Ind. Eng. Chem. Res.* **2018**, *57*, 2165.
[27] G. Gahleitner, *Int. J. Hydrogen Energy* **2013**, *38*, 2039.
[28] B. Kumar, M. Asadi, D. Pisasale, S. Sinha-Ray, B. A. Rosen, R. Haasch, J. Abiade, A. L. Yarin, A. Salehi-Khojin, *Nat. Commun.* **2013**, *4*, 2819.
[29] J. Wu, S. Ma, J. Sun, J. I. Gold, C. Tiwary, B. Kim, L. Zhu, N. Chopra, I. N. Odeh, R. Vajtai, A. Z. Yu, R. Luo, J. Lou, G. Ding, P. J. A. Kenis, P. M. Ajayan, *Nat. Commun.* **2016**, *7*, 13869.
[30] S. Verma, Y. Hamasaki, C. Kim, W. Huang, S. Lu, H.-R. M. Jhong, A. A. Gewirth, T. Fujigaya, N. Nakashima, P. J. A. Kenis, *ACS Energy Lett.* **2018**, *3*, 193.
[31] R. B. Kutz, Q. Chen, H. Yang, S. D. Sajjad, Z. Liu, I. R. Masel, *Energy Technol.* **2017**, *5*, 929.
[32] H. Yang, J. J. Kaczur, S. D. Sajjad, R. I. Masel, *J. CO2 Util.* **2017**, *20*, 208.
[33] Z. Liu, H. Yang, R. Kutz, R. I. Masel, *J. Electrochem. Soc.* **2018**, *165*, J3371.
[34] M. Dunwell, W. Luc, Y. Yan, F. Jiao, B. Xu, *ACS Catal.* **2018**, *8*, 8121.
[35] M. Dunwell, Q. Lu, J. M. Heyes, J. Rosen, J. G. Chen, Y. Yan, F. Jiao, B. Xu, *J. Am. Chem. Soc.* **2017**, *139*, 3774.
[36] Q. Lu, F. Jiao, *Nano Energy* **2016**, *29*, 439.
[37] Q. Lu, J. Rosen, Y. Zhou, G. S. Hutchings, Y. C. Kimmel, J. G. Chen, F. Jiao, *Nat. Commun.* **2014**, *5*, 3242.
[38] P. J. A. Kenis, A. Dibenedetto, T. Zhang, *ChemPhysChem* **2017**, *18*, 3091.

[39] A. Cyr, F. Chiltz, P. Jeanson, A. Martel, L. Brossard, J. Lessard, H. Ménard, *Can. J. Chem.* **2000**, *78*, 307.
[40] C. H. Lam, C. B. Lowe, Z. Li, K. N. Longe, J. T. Rayburn, M. A. Caldwell, C. E. Houdek, J. B. Maguire, C. M. Saffron, D. J. Miller, J. E. Jackson, *Green Chem.* **2015**, *17*, 601.
[41] Z. Li, S. Kelkar, L. Raycraft, M. Garedew, J. E. Jackson, D. J. Miller, C. M. Saffron, *Green Chem.* **2014**, *16*, 844.
[42] W. An, J. K. Hong, P. N. Pintauro, K. Warner, W. Neff, *J. Am. Oil Chem. Soc.* **1998**, *75*, 917.
[43] S. Verma, B. Kim, H.-R. Molly Jhong, S. Ma, P. J. A. Kenis, *ChemSusChem* **2016**, *9*, 1972.
[44] J. K. Kaldellis, D. Zafirakis, K. Kavadias, *Renewable Sustainable Energy Rev.* **2009**, *13*, 378.
[45] A. Jaiswal, *Renewable Sustainable Energy Rev.* **2017**, *72*, 922.
[46] R. Dufo-López, J. L. Bernal-Agustín, *Energy Convers. Manag.* **2015**, *91*, 394.
[47] A. Sakti, J. J. Michalek, E. R. H. Fuchs, J. F. Whitacre, *J. Power Sources* **2015**, *273*, 966.
[48] G. A. Olah, *Angew. Chem., Int. Ed.* **2005**, *44*, 2636.
[49] S. Mekhilef, R. Saidur, A. Safari, *Renewable Sustainable Energy Rev.* **2012**, *16*, 981.
[50] G. Apanel, E. Johnson, *Fuel Cells Bull.* **2004**, *2004*, 12.
[51] E. I. Zoulias, N. Lymberopoulos, *Renewable Energy* **2007**, *32*, 680.
[52] S. Prince-Richard, M. Whale, N. Djilali, *Int. J. Hydrogen Energy* **2005**, *30*, 1159.
[53] R. Dmello, J. D. Milshtein, F. R. Brushett, K. C. Smith, *J. Power Sources* **2016**, *330*, 261.
[54] R. M. Darling, K. G. Gallagher, J. A. Kowalski, S. Ha, F. R. Brushett, *Energy Environ. Sci.* **2014**, *7*, 3459.
[55] C. Ainscough, D. Peterson, E. Miller, S. Satyapal, *DOE Hydrogen and Fuel Cells Program Record*, HFC-PR-14004, US Department Of Energy, Washington, DC **2014**.
[56] B. James, W. Colella, J. Moton, G. Saur, T. Ramsden, *PEM Electrolysis H2A Production Case Study Documentation*, NREL/TP-5400-61387, National Renewable Energy Laboratory (NREL), Golden, CO **2013**.
[57] M. J. Orella, *Electrochemical-Economics*, https://github.com/michaelorella/electrochemical-economics (accessed: October 2019).
[58] S. Prasad, *J. Braz. Chem. Soc.* **2000**, *11*, 245.
[59] J. B. Dahmus, T. G. Gutowski, *Environ. Sci. Technol.* **2007**, *41*, 7543.
[60] K. Z. House, A. C. Baclig, M. Ranjan, E. A. van Nierop, J. Wilcox, H. J. Herzog, *Proc. Natl. Acad. Sci.* **2011**, *108*, 20428.
[61] F. Ausfelder, A. Bazzanella, *Hydrogen Science and Engineering: Materials, Processes, Systems and Technology*, John Wiley & Sons, Ltd, Weinheim, Germany **2016**, pp. 19–40.
[62] O. Schmidt, A. Gambhir, I. Staffell, A. Hawkes, J. Nelson, S. Few, *Int. J. Hydrogen Energy* **2017**, *42*, 30470.
[63] D. Pletcher, F. C. Walsh, *Industrial Electrochemistry*, Springer, Dordrecht, The Netherlands **1993**, pp. 294–330.
[64] B. Kim, F. Hillman, M. Ariyoshi, S. Fujikawa, P. J. A. Kenis, *J. Power Sources* **2016**, *312*, 192.
[65] L.-C. Weng, A. T. Bell, A. Z. Weber, *Phys. Chem. Chem. Phys.* **2018**, *20*, 16973.
[66] H.-R. Molly Jhong, S. Ma, P. J. Kenis, *Curr. Opin. Chem. Eng.* **2013**, *2*, 191.
[67] D. Pletcher, *Electrochem. Commun.* **2015**, *61*, 97.
[68] X. H. Chadderdon, D. J. Chadderdon, J. E. Matthiesen, Y. Qiu, J. M. Carraher, J.-P. Tessonnier, W. Li, *J. Am. Chem. Soc.* **2017**, *139*, 14120.
[69] S. Jung, A. N. Karaiskakis, E. J. Biddinger, *Catal. Today* **2019**, *323*, 26.
[70] Z. Li, S. Kelkar, C. H. Lam, K. Luczek, J. E. Jackson, D. J. Miller, C. M. Saffron, *Electrochim. Acta* **2012**, *64*, 87.
[71] P. Nilges, U. Schröder, *Energy Environ. Sci.* **2013**, *6*, 2925.
[72] L. Liu, H. Liu, W. Huang, Y. He, W. Zhang, C. Wang, H. Lin, *J. Electroanal. Chem.* **2017**, *804*, 248.
[73] K. J. Carroll, T. Burger, L. Langenegger, S. Chavez, S. T. Hunt, Y. Román-Leshkov, F. R. Brushett, *ChemSusChem* **2016**, *9*, 1904.
[74] Z. Li, M. Garedew, C. H. Lam, J. E. Jackson, D. J. Miller, C. M. Saffron, *Green Chem.* **2012**, *14*, 2540.
[75] B. Huang, C. Durante, A. A. Isse, A. Gennaro, *Electrochem. Commun.* **2013**, *34*, 90.
[76] C. H. Lam, S. Das, N. C. Erickson, C. D. Hyzer, M. Garedew, J. E. Anderson, T. J. Wallington, M. A. Tamor, J. E. Jackson, C. M. Saffron, *Sustainable Energy Fuels* **2017**, *1*, 258.
[77] P. Popovic, *ICIS Chem. Bus.* **2018**, *293*, 39.
[78] J. D. Milshtein, A. P. Kaur, M. D. Casselman, J. A. Kowalski, S. Modekrutti, P. L. Zhang, N. H. Attanayake, C. F. Elliott, S. R. Parkin, C. Risko, F. R. Brushett, S. A. Odom, *Energy Environ. Sci.* **2016**, *9*, 3531.